RESEARCH PAPER

Effects of Joule heating and viscous dissipation on Casson nanofluid flow over a stretched sheet with chemical reaction

Madan Mohan Muduly [a], Pravat Kumar Rath [b], Pallab Kar [c], Kharabela Swain [c] [*]

[a] *Department of Mathematics, OUTR, Bhubaneswar-751003, India*
[b] *Department of Mathematics, BRM IIT, Bhubaneswar-751010, India*
[c] *Department of Mathematics, Gandhi Institute for Technology, Bhubaneswar-752054, India*

Abstract

Nanofluids find numerous applications in thermal engineering and industrial processes due to their effective thermal conductivity property compared to regular fluids. A nanofluid consists of containing nanometer-sized particles, called nanoparticles of metals, oxides, carbides, or carbon nanotubes etc. with water, ethylene glycol, and oil etc. serve as base fluids. The present study takes care of effects of Brownian motion and thermophoresis on unsteady Casson fluid flow, heat and mass transfer over a stretching sheet embedded in a porous medium. Moreover, the flow phenomena are subjected to heat source, thermal radiation, viscous dissipation, Joule heating and are associated with the diffusion of chemically reactive nanoparticles to base fluid. These two thermo mechanical aspects draw a little attention of the researchers as reported in literature. The governing equations of flow model admit similarity solution and are reduce to non-linear ordinary differential equations (ODEs) applying suitable similarity transformation and are solved numerically using Runge-Kutta-Fehlberg method with MATLAB code. The interesting outcomes are recorded as follows: The formation of inverted boundary layer, the consequence of flow reversal, is due to overpowering of shearing effect of the rigid bounding surface over the free stream stretching in the absence of suction. The higher magnetic field intensity as well as unsteady flow parameter leads to increasing skin friction coefficient may lead to flow reversal. Hence, regulating these parameters is a suggesting measure. The low Brownian motion in conjunction with high thermophoresis leads to upsurge of thermal energy (hike in temperature profile) near the bounding surface. The presence of nanoparticles considered in the base fluid, deduces the shearing stress at the plate surface is a desired outcome to avoid flow reversal.

Keywords: MHD; heat and mass transfer; Casson fluid; thermophoresis; Brownian motion; chemical reaction.

1. Introduction

A number of technical processes such as polymer extraction in a melt spinning process, glass blowing,

---

[*] Corresponding author. *E-mail address:* kharabela1983@gmail.com

continuous casting of metals, etc. affect the flow of an incompressible Newtonian or non-Newtonian fluid over a stretched surface significantly. A flow caused by extending a surface had a closed-form similarity solution [1]. Mahapatra and Gupta [2] and Misra and Sinha [3] worked on the stagnation point flow on a stretching sheet. The work [3] bears a favor of biological application.

Nomenclature

u, v	Velocities along x and y direction respectively	k^*	Absorption coefficient
a	Stretching rate	T	Temperature
b	Strength of stagnation flow	C	Nanoparticle volume fraction
t	Time	U_e	Ambient fluid velocity
B_0	Magnetic field strength	T_w	Temperature of the wall
M	Magnetic parameter	T_∞	Ambient temperature
K	Porosity parameter	C_∞	Ambient concentration
Kc	Chemical reaction parameter	***Greek Symbols***	
Pr	Prandtl number	η	Similarity variable
Nb	Brownian motion parameter	σ	Electrical conductivity
Nt	Thermophoresis parameter	ψ	Stream function
Sc	Schmidt number	λ	Positive constant
R	Radiation parameter	γ	Casson parameter
S	Unsteadiness parameter	β	Stretching ratio parameter
Kc	Chemical reaction parameter	σ^*	Stefan-Boltzmann constant
D_B	Brownian diffusion coefficient	α	Thermal diffusivity
D_T	Thermophoresis diffusion coefficient	τ	Ratio of the nanoparticle heat capacity to the base fluid heat capacity
c_p	Specific heat at constant temperature	$(\rho c)_f$	Heat parameter of base fluid
Q^*	heat source/sink coefficient	$(\rho c)_p$	Heat parameter of nanoparticle
k	Thermal conductivity coefficient	μ_f	Dynamic viscosity of base fluid
K^*	Permeability of the medium	υ_f	Kinematic viscosity of base fluid
Q	Heat source/sink parameter	ρ_f	Density of base fluid

The Casson fluid is a good representative of human blood with non-Newtonian property. Beyond a critical stress value, it behaves like a Newtonian fluid. Bhattacharyya [4] examined the stagnation point flow of Casson fluid past a stretched surface. Ibrahim et al. [5] studied the effects of radiation and chemical reaction on non-Newtonian fluid flow over a stretching sheet. Kumar and Srinivas [6] studied the unsteady flow of chemically reacting Casson fluid over an inclined porous stretching sheet. El-Aziz and Afify [7] investigated the Casson fluid flow over a stretching sheet considering Hall current, an electromagnetic phenomenon. Das et al. [8] considered chemically reactive double-diffusive Casson fluid past a flat plate in porous medium. Kumar et al. [9] studied the effect of thermal radiation on MHD Casson fluid flow over an exponentially stretching curved sheet. Nayak et al. [10] examined the stability analysis on MHD stagnation point flow of Casson fluid over the stretching surface with slip velocity. Further, Kumar et al. [11] studied the pulsating flow of Casson nanofluid in a vertical porous space. Gireesha et al.

[12] analysed the heat transfer of Casson fluid flow in an inclined porous microchannel with viscous and Joule heating. Kumar and Srinivas [13] studied the Eyring-Powell nanofluid flow over an inclined permeable stretching sheet. El-Aziz and Afify [14] considered the Hall current effect on MHD slip flow of Casson nanofluid over a stretching sheet with zero nanoparticle mass flux. Many authors [15-20] have studied the influences of physical parameters on Casson fluid flow over a stretching sheet considering different boundary conditions.

The effect of thermal radiation on the boundary layer flow is relevant to many engineering challenges, particularly, in high temperature field. Due to the impact of thermal radiation on the rate of cooling, it is crucial in regulating the quality of the final product. Swain et al. [21] investigated the flow of Williamson nanofluid considering thermal radiation. VeeraKrishna [22] examined the effect of Newtonian heating on Casson hybrid nanofluids past an infinite oscillating vertical porous plate. Azam et al. [23] studied the radiation and viscous dissipation effects on Casson nanoliquid over a moving cylinder with activation energy. Some important works on thermal radiation effect had been done by the researchers [24, 25].

Mohammadi et al. [26-67] studied the thermo-mechanical vibration investigation of annular and circular graphene sheet embedded in an elastic medium using the nonlocal continuum plate model. Ibrahim and Makinde [68, 69] studied the MHD stagnation point flow and heat transfer of Casson nanofluid past a stretching sheet with slip boundary conditions. Makinde et al. [70] examined the stagnation point flow of nanofluid over a stretching surface with chemical reaction. Satya Narayana et al. [71] considered the flow of visco-elastic nanofluid over a heated surface. Rehman et al. [72] observed the effect of Joule heating on the flow of Eyring-Powell fluid induced by an inclined cylindrical surface. Mehmood et al. [73] studied the stagnation point flow of Casson fluid over a stretched horizontal Riga plate.

The novelties of the present study are many folds. The inclusion of viscous dissipation arising out of material/rheological property of the Casson fluid due to inter layer friction of the flowing fluid dissipating thermal energy. The effect of Joule heating affecting the thermal energy arising out of electromagnetic interaction due to applied magnetic field. Nevertheless consideration of chemical reaction arising out of chemically reactive species which adds to the mass diffusion processes of the present analysis. Most importantly, Das et al. [74] have not considered the effect of electrical conductivity of the Casson fluid with the interaction of magnetic field which gives rise to a resistive external body forces affecting the momentum transport processes. Moreover, they have not considered the embedding medium of the stretching surface most likely porous medium, which relates to many physical and biological system. The inclusion ascribes to another body force accounted for with the help of linear Darcy law valid for slow flow comparable to mild stretching of the sheet aptly represent biological system. The similarity solution of the unsteady complex coupled partial differential equations with time and space dependent boundary conditions renders mathematical impasse to analytical solution paving the way to numerical solution being accomplished by the shooting technique with MATLAB code.

2. Formulation of the problem

The unsteady two dimensional flow of an electrically conducting Casson nanofluid flow over an elongated sheet embedded in a porous medium is investigated. The plate is placed along x-axis and y-axis is normal to it (Fig. 1). The flow confined to the plane $y > 0$, is due to elongated bounding surface and free stream. The rheological equation of state for an isotropic and incompressible flow of a Casson fluid [16] is expressed as:

$$\tau_{ij} = \begin{cases} 2\left(\mu_B + \dfrac{p_y}{\sqrt{2\pi}} \right)e_{ij}, \pi > \pi_c \\[4mm] 2\left(\mu_B + \dfrac{p_y}{\sqrt{2\pi_c}} \right)e_{ij}, \pi < \pi_c \end{cases}$$

where $e_{ij} = \dfrac{1}{2}\left(\dfrac{\partial u_i}{\partial x_j} + \dfrac{\partial u_j}{\partial x_i} \right)$ is the rate of strain tensor, τ_{ij} is the component of stress tensor, μ_B is the Casson coefficient of viscosity, $\pi = e_{ij}e_{ij}$ is the product of the rate of strain tensor with itself, π_c is the critical value of the product of the rate of strain tensor with itself, p_y is the yield stress of the fluid.
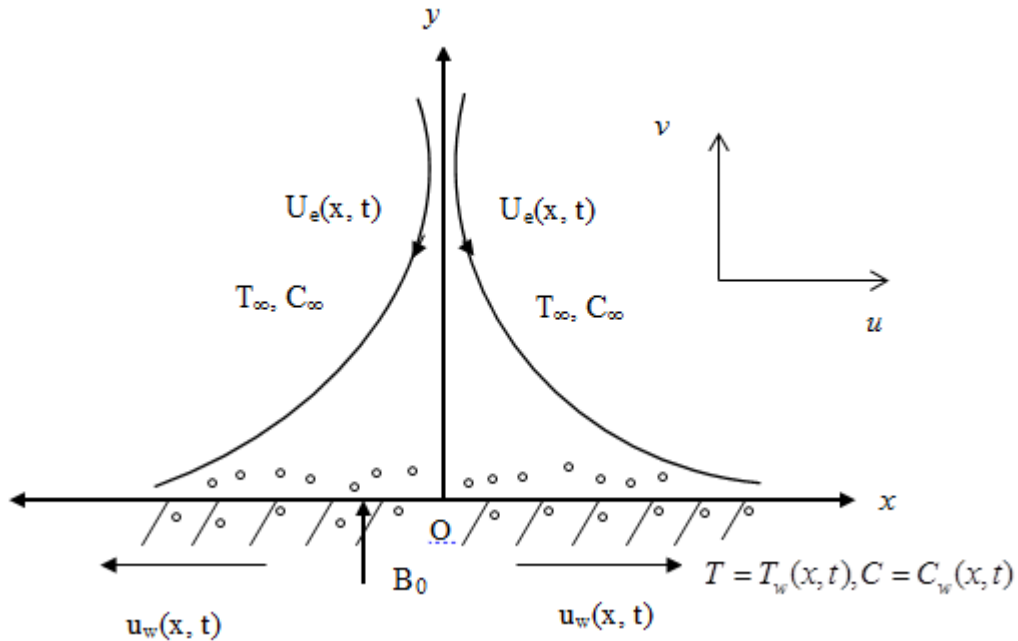
Fig. 1 Flow geometry

The continuity, momentum, energy and concentration equations with prescribed boundary conditions [74] and Rosseland approximation [75] are given by

$$\frac{\partial u}{\partial x} + \frac{\partial v}{\partial y} = 0 \tag{1}$$

$$\frac{\partial u}{\partial t} + u\frac{\partial u}{\partial x} + v\frac{\partial u}{\partial y} = \frac{\partial U_e}{\partial t} + U_e\frac{\partial U_e}{\partial x} + \upsilon_f\left(1+\frac{1}{\gamma}\right)\frac{\partial^2 u}{\partial y^2} - \frac{\sigma B_0^2}{\rho_f}(u-U_e) - \frac{\upsilon_f}{K_p^*}(u-U_e) \tag{2}$$

$$\frac{\partial T}{\partial t} + u\frac{\partial T}{\partial x} + v\frac{\partial T}{\partial y} = \left(\alpha + \frac{16\sigma^* T_\infty^3}{3k^*}\right)\frac{\partial^2 T}{\partial y^2} + \tau\left[D_B\frac{\partial T}{\partial y}\frac{\partial C}{\partial y} + \frac{D_T}{T_\infty}\left(\frac{\partial T}{\partial y}\right)^2\right]$$

$$+ \frac{\sigma B_0^2(u-U_e)^2}{(\rho c)_f} + \frac{\mu_f}{(\rho c)_f}\left(1+\frac{1}{\gamma}\right)\left(\frac{\partial u}{\partial y}\right)^2 + \frac{Q^*}{(\rho c)_f}(T-T_\infty) \tag{3}$$

$$\frac{\partial C}{\partial t} + u\frac{\partial C}{\partial x} + v\frac{\partial C}{\partial y} = D_B\frac{\partial^2 C}{\partial y^2} + \left(\frac{D_T}{T_\infty}\right)\frac{\partial^2 T}{\partial y^2} - Kc(C-C_\infty) \tag{4}$$

$$\left.\begin{array}{l} u = u_w(x,t) = \dfrac{ax}{1-\lambda t}, v = 0, T = T_w(x,t), C = C_w(x,t) \ \ at \ y = 0 \\[4mm] u = U_e(x,t) = \dfrac{bx}{1-\lambda t}, T \to T_\infty, C \to C_\infty \qquad\qquad as \ y \to \infty \end{array}\right\} \tag{5}$$

Here, stretching velocity $u_w(x,t) = \dfrac{ax}{1-\lambda t}$, free stream velocity $U_e(x,t) = \dfrac{bx}{1-\lambda t}$, and the wall temperature (T_w) and nanoparticle volume fraction (C_w) are given by $T_w(x,t) = T_\infty + T_0\left[\dfrac{ax^2}{(1-\lambda t)}\right]$ and

$C_w(x,t) = C_\infty + C_0\left[\dfrac{ax^2}{(1-\lambda t)}\right]$ respectively.

In order to convert the coupled PDEs to ODEs, the following similarity variables, transformations and

parameters are introduced. This is also supported by plane stagnation point flow [76].

$$
\begin{aligned}
& \eta = \sqrt{\frac{a}{\upsilon_f(1-\lambda t)}}\, y, \psi = \sqrt{\frac{a\upsilon_f}{(1-\lambda t)}}\, xf(\eta), u = \frac{\partial \psi}{\partial y}, v = -\frac{\partial \psi}{\partial x}, \\
& T = T_\infty + T_0\left[\frac{ax^2}{(1-\lambda t)^2}\right]\theta(\eta), C = C_\infty + C_0\left[\frac{ax^2}{(1-\lambda t)^2}\right]\phi(\eta), \\
& S = \frac{\lambda}{a}, \beta = \frac{b}{a}, \mathrm{Pr} = \frac{\upsilon_f}{\alpha}, R = \frac{4T_\infty^3\sigma^*}{k^*k}, M = \frac{\sigma B_0^2}{\rho_f a}, K_p = \frac{\upsilon_f}{K_p^* a}, \\
& Sc = \frac{\upsilon_f}{D_B}, Q = \frac{Q^*}{a(\rho c_p)_f}, Kc = \frac{Kc^*}{a}, Nb = \frac{\tau D_B(C_w - C_\infty)}{\upsilon_f}, \\
& Nt = \frac{\tau D_T(T_w - T_\infty)}{\upsilon_f T_\infty}, Ec = \frac{u_w^2}{(c_p)_f(T_w - T_\infty)}
\end{aligned}
\right\}
\tag{6}
$$

Equation (1) is identically satisfied and the equations (2) - (5) yield the preferred form:

$$
\left(1+\frac{1}{\gamma}\right)f''' + ff'' - f'^2 - (M+K_p)(f'-\beta) + \beta^2 - S\left(\frac{1}{2}\eta f'' + f' - \beta\right) = 0
\tag{7}
$$

$$
\frac{1}{\mathrm{Pr}}(1+R)\theta'' + f\theta' - 2f'\theta + Nb\theta'\phi' + Nt\theta'^2 + MEc(f'-\beta)^2
$$
$$
+ Ec\left(1+\frac{1}{\gamma}\right)f''^2 + Q\theta - S\left(\frac{1}{2}\eta\theta' + 2\theta\right) = 0
\tag{8}
$$

$$
\phi'' + Sc\left[f\phi' - 2f'\phi - Kc\phi - S\left(\frac{1}{2}\eta\phi' + 2\phi\right)\right] + \frac{Nt}{Nb}\theta'' = 0
\tag{9}
$$

$$
\left.\begin{aligned}
& f'(\eta)=1, f(\eta)=0, \theta(\eta)=1, \phi(\eta)=1 \quad at\ \eta=0 \\
& f'(\eta)=\beta, \theta(\eta)=0, \phi(\eta)=0 \qquad\qquad as\ \eta\to\infty
\end{aligned}\right\}
\tag{10}
$$

The dimensionless local skin friction coefficient C_f, the local Nusselt number Nu_x and the local Sherwood number Sh_x which are defined as follows

$$
C_f = \frac{\mu}{\rho_f U_w^2}\left(\frac{\partial u}{\partial y}\right)_{y=0} \Rightarrow \mathrm{Re}_x^{0.5}C_{fx} = \left(1+\frac{1}{\gamma}\right)f''(0)
\tag{11}
$$

$$
Nu_x = \frac{-x}{(T_w - T_\infty)}\left[\frac{\partial T}{\partial y} - \frac{4\sigma^*}{3k^{'*}}\left(\frac{\partial T^4}{\partial y}\right)\right]_{y=0} \Rightarrow \mathrm{Re}_x^{-0.5}Nu_x = -(1+R)\theta'(0)
\tag{12}
$$

$$
Sh_x = \frac{-x}{(C_w - C_\infty)}\left(\frac{\partial C}{\partial y}\right)_{y=0} \Rightarrow \mathrm{Re}_x^{-0.5}Sh_x = -\phi'(0)
\tag{13}
$$

The steady-state flow is recovered when $S = 0$.

3. Method of solution

The set of non-linear coupled ordinary differential equations (7) - (10) have been solved numerically by Runge-Kutta-Fehlberg method with shooting technique using MATLAB software with step size of $\nabla\eta = 0.01$ and error bound 10^{-6} in all cases. Advantages of this method are that the coupled nonlinear ODEs are transformed to a set of linear first order ODEs with the introduction of the new variables. Secondly, the boundary value problem gets

transformed to initial value problem by providing guess values to unknown initial values as required by the problem to be solved. The guess values are corrected by the shooting method to tally with the specified boundary conditions at the other boundary. Once the guess values are corrected with required number of iterations, then the forward integration is carried out to give the numerical solutions of the desired points comprising interval. The limitations are: Not all the PDEs, representing the governing equations, do not admit similarity transformations and cannot be transformed to ODEs. Only specific types of flow problems admit similarity transformations and hence similar solutions. There might be dual solutions to a specific problem, if exists, then which one is stable or unstable that is to be decided upon and discussed. To assess the accuracy of the present code and validity check, the numerical values of skin friction coefficient $f''(0)$ for different values of β are presented in Table 1 when $M = Kp = S = 0, \gamma \to \infty.$

TABLE 1 Comparison of $f''(0)$ for different values of β

β	$f''(0)$		
	Present study	Swain et al. [67]	Das et al. [66]
0.1	-0.9696514	-0.96965625	-0.969328
0.2	-0.9181601	-0.91816450	-0.918098
0.5	-0.6672609	-0.66726432	-0.667301
2	2.0175025	2.01750252	2.017467
3	4.7292808	4.72928082	4.729406

4. Results and discussion

For numerical computation, we have considered some values of the parameters as fixed i.e. $M = K_p = \beta = \gamma = 0.5, S = Kc = 0.3, Sc = 2, R = Q = Ec = Nb = Nt = 0.1,$ and $\Pr = 5$ unless otherwise specified.

Table 2 shows the variations of $-f''(0)$ for different values of parameters. It is observed that when values of other parameters are fixed, the wall shear stress $\{-f''(0)\}$ increases with the increase in the values of M and S, whereas it decreases with increase in the values of β and γ. Physically, it means that higher values of magnetic intensity decrease the shear stress at the bounding surface. Further, it is concluded that higher the unsteadiness, greater the shearing stress at the bounding surface. From Table 3 it is seen that the rates of heat transfer and solutal concentration at the bounding surface increase with unsteady parameter whereas rate of heat transfer decreases and rate of solutal concentration increases with higher values of M. It is also observed that $-\theta'(0)$ increases with increase in strength of heat sink $(Q < 0)$ but $-\phi'(0)$ decreases. Further, it is seen that heat source $(Q > 0), Sc$ and destructive chemical reaction parameter $(Kc > 0)$ have opposite effects on $-\theta'(0)$ and $-\phi'(0)$, compared to that of constructive chemical reaction parameter $(Kc < 0)$ and heat source $(Q > 0)$. It is interesting to note that the rate of mass transfer at the wall shows an opposite effect compared to rate of heat transfer for all the parameter except unsteadiness parameter (S). This outcome may be attributed to the fact that higher thermal energy enhances the solutal diffusion causing the fall of concentration level and hence, the flux at the wall. It is interesting to note that the presence of nanoparticles in the base fluid reduces the shearing force at the plate surface, hence imposing stability or preventing backflow in the downstream.

From Fig. 2 it is seen that the boundary layer is formed when $\beta > 1$ and inverted boundary layer is formed when $\beta < 1$ whereas no boundary layer is formed for $\beta = 1$. The magnetic parameter decreases the velocity profile due to resistive Lorentz force however; the effect is reversed in case of inverted boundary layer. Further, the presence of porous matrix and moderate values of Casson parameter are to reduce the velocity, resulting a thinner boundary layer (Fig. 3). Inside the boundary layer, the pressure gradient dominates the momentum transfer of the outer shear flow. Therefore, shear induced component of the free stream shear flow inside the boundary layer is less than the inviscid value. This results in flow reversal in the absence of suction. Reza and Gupta [77] The formation of the inverted boundary layer in the present study is the outcome of flow reversal due to over powering of shearing effect

of the boundary over free stream in the absence of suction.
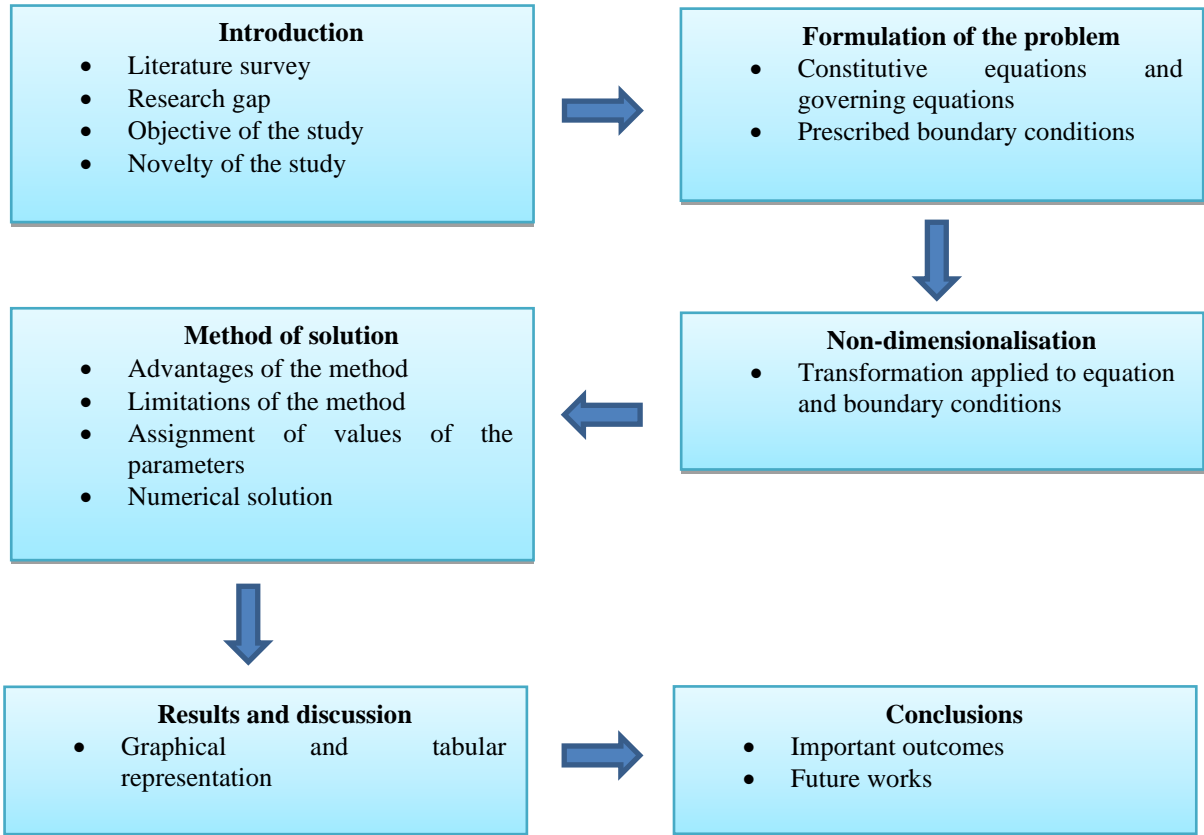
Flow chart

Introduction
- Literature survey
- Research gap
- Objective of the study
- Novelty of the study

Formulation of the problem
- Constitutive equations and governing equations
- Prescribed boundary conditions

Non-dimensionalisation
- Transformation applied to equation and boundary conditions

Method of solution
- Advantages of the method
- Limitations of the method
- Assignment of values of the parameters
- Numerical solution

Results and discussion
- Graphical and tabular representation

Conclusions
- Important outcomes
- Future works

Table 2 Computation of $\left\{-f''(0)\right\}$

when $K_p = 0.5, Kc = 0.3, Sc = 2, \Pr = 5, R = Q = Ec = Nb = Nt = 0.1$

M	β	S	γ	$-f''(0)$
0.1	0.1	0	0.5	2.070225
0.5				2.290439
1				2.540362
	0.3			2.086459
	0.5			1.565345
		0.5		1.650139
		1		1.732104
			1	1.414217
			2	1.224745

Table 3 Computation of $-\theta'(0)$ and $-\phi'(0)$ when $K_p = \beta = \gamma = 0.5, \Pr = 5, R = Ec = Nb = Nt = 0.1$

M	S	Q	Sc	Kc	$-\theta'(0)$	$-\phi'(0)$
0.1	0.1	0.1	2	0.1	2.915176	0.844825
0.5					2.893939	0.849222
1					2.868720	0.855275
	0.3				3.090879	0.892068
	0.5				3.299090	0.927975

0.5				3.033451	1.122957
1				2.670987	1.382402
-0.3				3.547863	0.742159
-0.5				3.666891	0.652257
0.1	3			3.208601	1.752369
	5			3.093658	2.978601
		0.5		3.068714	3.288434
		0		3.100417	2.897159
		-0.3		3.122186	2.641721
		-0.5		3.138127	2.460946

Figs. 4-6 depict the temperature profile for various values of Q, Ec, Nb and Nt. It is seen that temperature increases with the strength of heat source $(Q > 0)$ but decreases with heat sink $(Q < 0)$. Further, both Eckert number (Ec) and radiation parameter (R) increase the temperature as an increase in Ec and R contribute to higher thermal energy (Figs. 4 and 5). As Eckert number (Ec) is the measure of addition of heat energy due to viscous dissipation, so that higher value of Ec gives rises to rise in temperature. Fig. 6 shows that an increase in Brownian motion parameter (Nb), increases the thermal energy, and hence the rise in temperature is observed but the reverse effect is observed in case of solutal concentration. Moreover, thermophoresis parameter (Nt) enhances both temperature and volume fraction due to thermophoretic effect. It is interesting to note that for low Brownian motion and high thermophoresis resulted in hike in temperature near the plate surface (Fig. 7).

Fig. 8 depicts the concentration profile for various values of chemical reaction parameter (Kc). It is observed that the concentration level deplete with higher rate of destructive reaction $(Kc > 0)$ and Schmidt number (Sc) but opposite effect is marked for constructive reaction parameter $(Kc < 0)$. Physically, both destructive reaction and Schmidt number (heavier species) decelerates the mass diffusion contributing to thinner solutal boundary layer (Fig. 9). Finally, it is important to note that the unsteadiness of the flow reduces the momentum transport and mass concentration but enhances the thermal energy irrespective of the effects of other parameters.
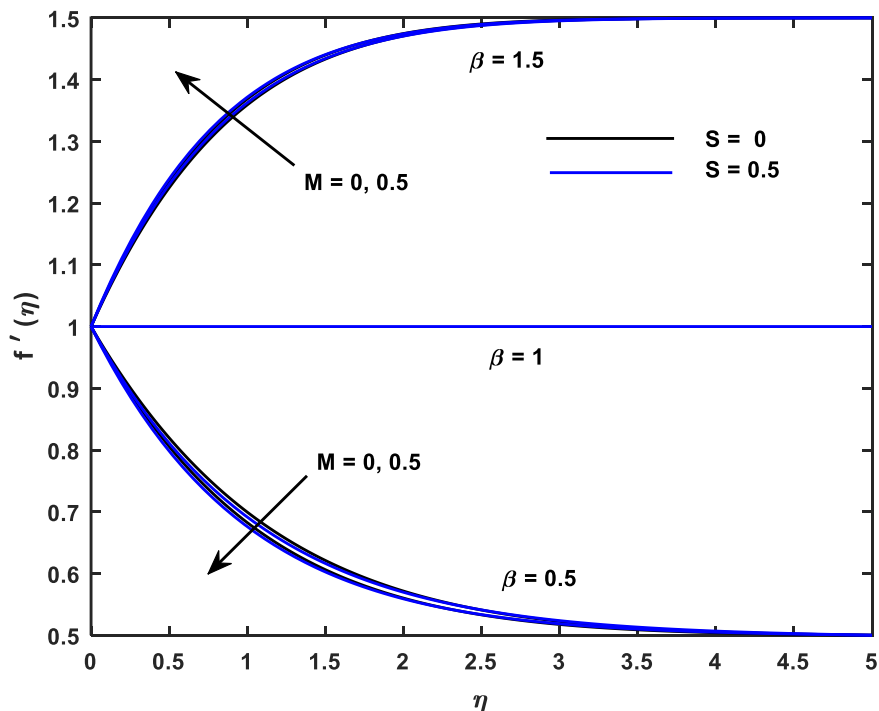

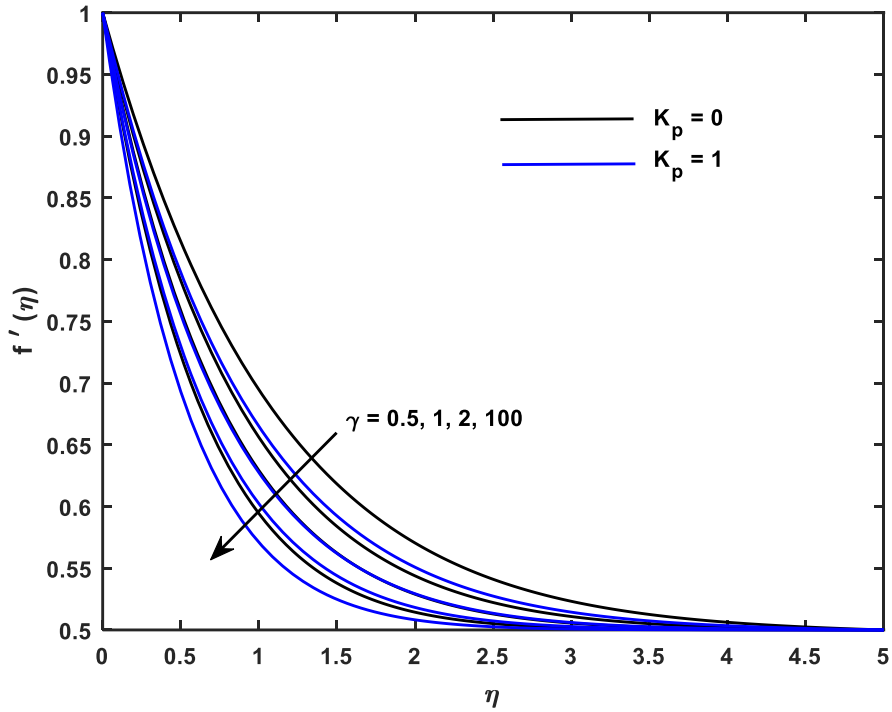Fig. 2 Velocity profiles for various values of M and β

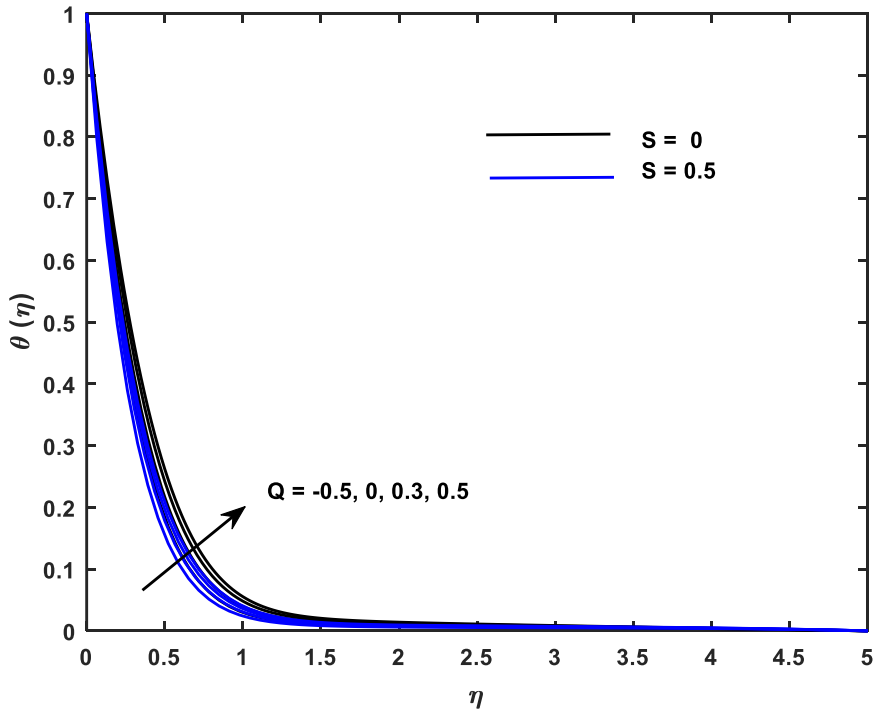Fig. 3 Velocity profiles for various values of γ and K_p

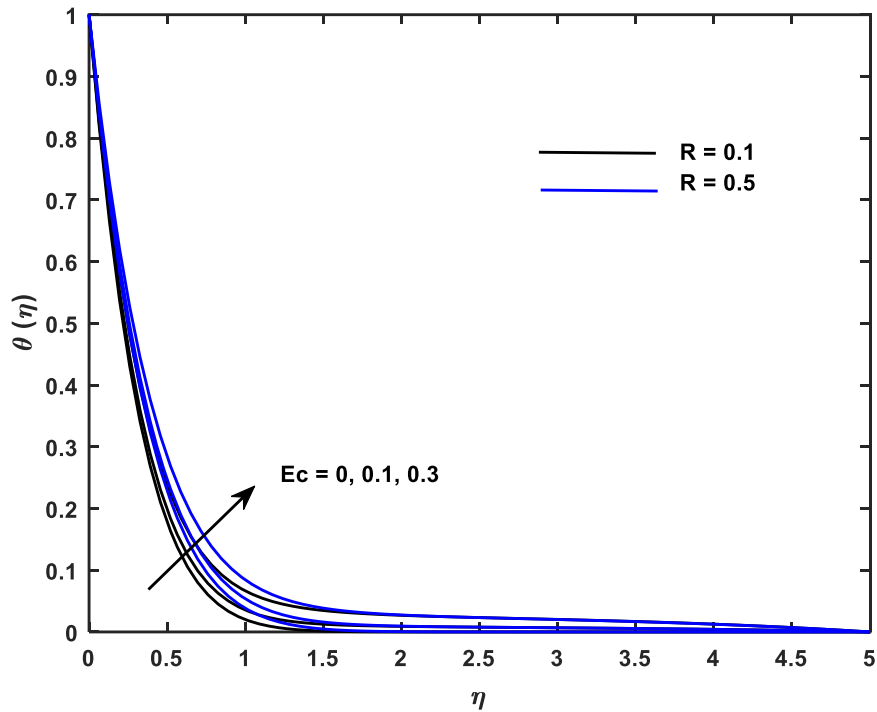Fig. 4 Temperature profiles for various values of Q

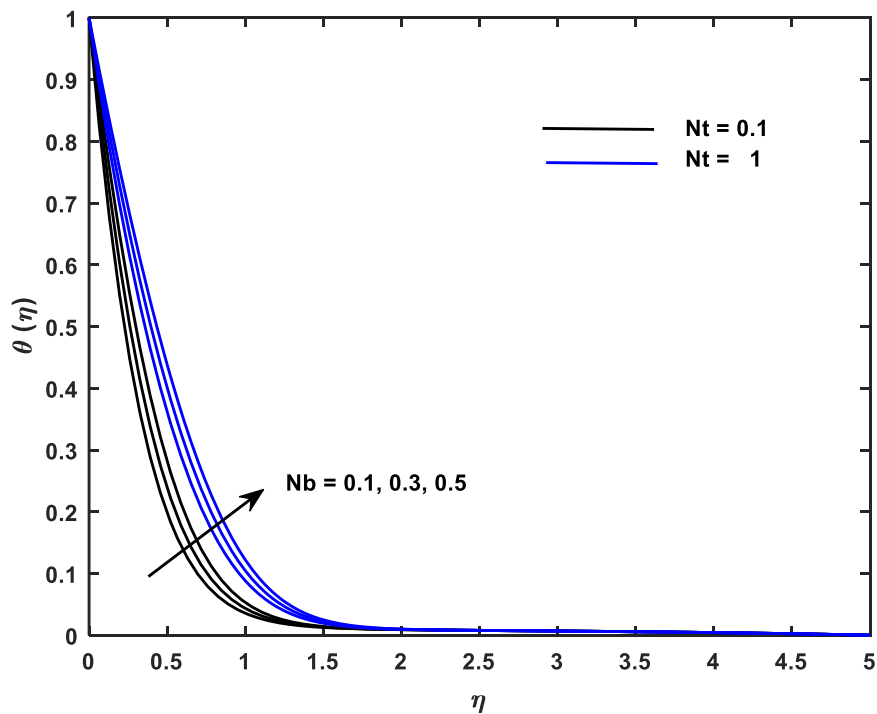Fig. 5 Temperature profiles for various values of Ec and R

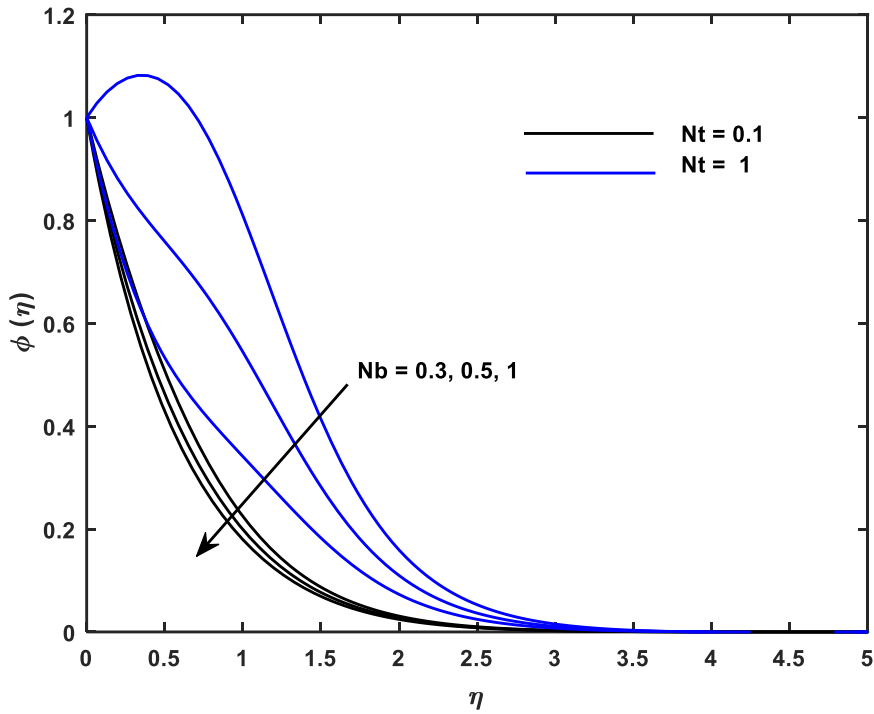Fig. 6 Temperature profiles for various values of Nb and Nt

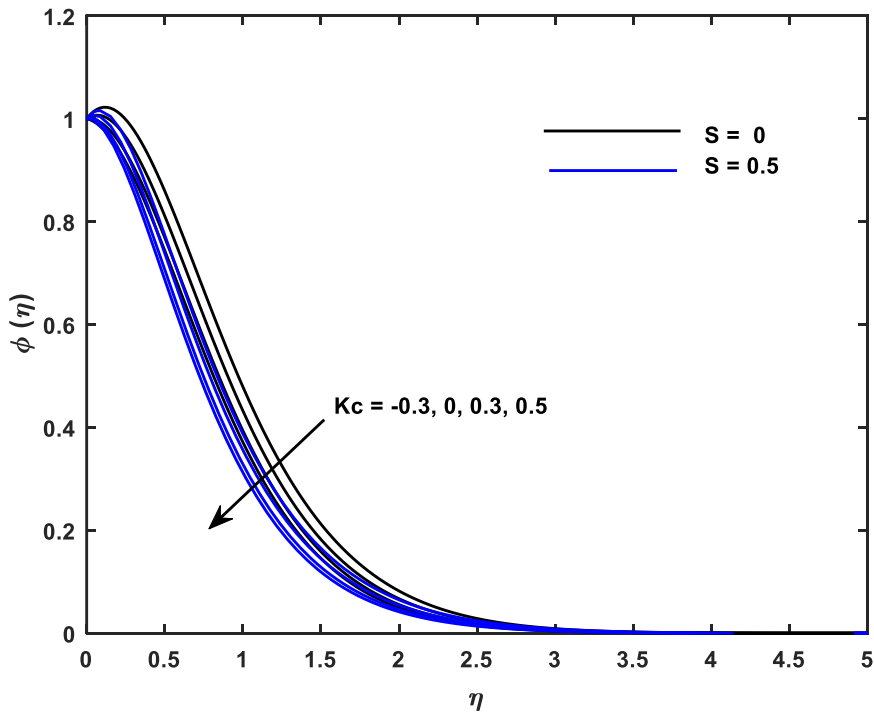Fig. 7 Concentration profiles for various values of Nb and Nt

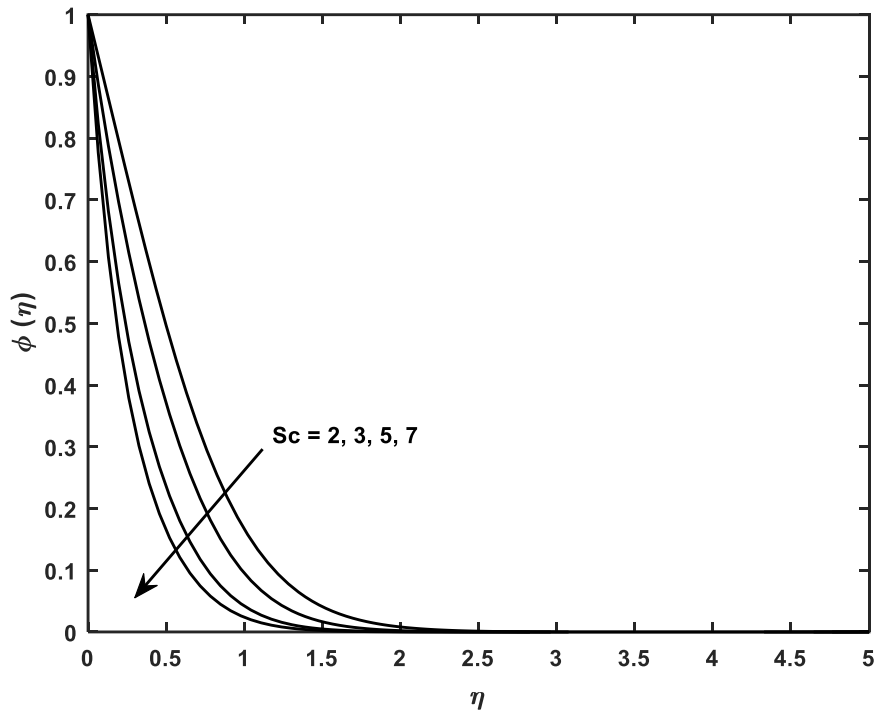Fig. 8 Concentration profiles for various values of Kc

Fig. 9 Concentration profiles for various values of *Sc*

5. Conclusions

From the present study the important finding are reported as follows:

- Formation of boundary layer is altered depending upon the value of stretching ratio parameter i.e. over powering of free stream stretching to bounding surface stretching. Physically, it indicates the reversal of momentum transport in the flow domain presented in velocity distribution graph.
- By the relative shearing impact of the plate and the free stream, the formation of the inverted boundary layer can be controlled.
- Higher values of magnetic field intensity as well as unsteady parameter lead to increasing skin friction coefficient. Thus, it is suggested that the necessary control may be enforced by controlling the voltage in the electric circuit or otherwise restrict/limit the magnetic intensity and unsteadiness to reduce the growth of skin friction to avoid back flow.
- Brownian motion favours the escalation of temperature distribution but sets in an impasse for the rise in level of concentration.
- The unsteadiness of the flow reduces the momentum transport and mass concentration but enhances the thermal energy irrespective of the effects of other parameters.
- Thermophoresis favours the rise in both temperature and volume fraction of the nanofluid in the entire flow domain.
- The presence of nanoparticles in the base fluid reduces the shearing stress at the plate surface so as to avoid back flow.
- The rate of heat transfer increases with increase in strength of heat sink but mass transfer decreases.
- Destructive and constructive chemical reactions have opposite effects to each other on heat and mass transfer of nanofluid.

Limitations: The present analysis is having following limitations.

- Consideration of space dependent linear stretching.
- Consideration of slow/seepage flow in the embedded porous medium.

Future work:

- Future work may be carried out by replacing the linear stretching with non-linear stretching having power indexed space variable $\left(x^n \right)$ which occurs in industrial applications very often.

- The linear Darcy law may be replaced by non-linear laws (Brinkmann, Forchheimer etc.) to account for moderately high flows.

References

[1]   L. J. Crane, Flow past a stretching plate, *Zeitschrift für angewandte Mathematik und Physik ZAMP,* Vol. 21, No. 4, pp. 645-647, 1970.

[2]   T. Mahapatra, A. Gupta, Heat transfer in stagnation-point flow towards a stretching sheet, *Heat and Mass transfer,* Vol. 38, No. 6, pp. 517-521, 2002.

[3]   J. Misra, A. Sinha, Effect of thermal radiation on MHD flow of blood and heat transfer in a permeable capillary in stretching motion, *Heat and Mass Transfer,* Vol. 49, No. 5, pp. 617-628, 2013.

[4]   K. Bhattacharyya, MHD stagnation-point flow of Casson fluid and heat transfer over a stretching sheet with thermal radiation, *Journal of thermodynamics,* Vol. 2013, 2013.

[5]   S. M. Ibrahim, P. V. Kumar, O. D. Makinde, Chemical reaction and radiation effects on non-Newtonian fluid flow over a stretching sheet with non-uniform thickness and heat source, in *Proceeding of,* Trans Tech Publ, pp. 319-331.

[6]   C. K. Kumar, S. Srinivas, Influence of Joule heating and thermal radiation on unsteady hydromagnetic flow of chemically reacting Casson fluid over an inclined porous stretching sheet, *Special Topics & Reviews in Porous Media: An International Journal,* Vol. 10, No. 4, 2019.

[7]   M. Abd El-Aziz, A. A. Afify, MHD Casson fluid flow over a stretching sheet with entropy generation analysis and Hall influence, *Entropy,* Vol. 21, No. 6, pp. 592, 2019.

[8]   M. Das, G. Mahanta, S. Shaw, S. Parida, Unsteady MHD chemically reactive double-diffusive Casson fluid past a flat plate in porous medium with heat and mass transfer, *Heat Transfer—Asian Research,* Vol. 48, No. 5, pp. 1761-1777, 2019.

[9]   K. Anantha Kumar, V. Sugunamma, N. Sandeep, Effect of thermal radiation on MHD Casson fluid flow over an exponentially stretching curved sheet, *Journal of Thermal Analysis and Calorimetry,* Vol. 140, No. 5, pp. 2377-2385, 2020.

[10]   M. Nayak, G. Mahanta, K. Karmakar, P. Mohanty, S. Shaw, Effects of thermal radiation and stability analysis on MHD stagnation casson fluid flow over the stretching surface with slip velocity, in *Proceeding of,* AIP Publishing LLC, pp. 020045.

[11]   C. K. Kumar, S. Srinivas, A. S. Reddy, MHD pulsating flow of Casson nanofluid in a vertical porous space with thermal radiation and Joule heating, *Journal of Mechanics,* Vol. 36, No. 4, pp. 535-549, 2020.

[12]   B. Gireesha, C. Srinivasa, N. Shashikumar, M. Macha, J. Singh, B. Mahanthesh, Entropy generation and heat transport analysis of Casson fluid flow with viscous and Joule heating in an inclined porous microchannel, *Proceedings of the Institution of Mechanical Engineers, Part E: Journal of Process Mechanical Engineering,* Vol. 233, No. 5, pp. 1173-1184, 2019.

[13]   B. Kumar, S. Srinivas, Unsteady hydromagnetic flow of Eyring-Powell nanofluid over an inclined permeable stretching sheet with joule heating and thermal radiation, *Journal of applied and computational mechanics,* Vol. 6, No. 2, pp. 259-270, 2020.

[14]   M. A. El-Aziz, A. Afify, Effect of Hall current on MHD slip flow of Casson nanofluid over a stretching sheet with zero nanoparticle mass flux, *Thermophysics and Aeromechanics,* Vol. 26, No. 3, pp. 429-443, 2019.

[15]   S. G. Bejawada, Y. D. Reddy, W. Jamshed, K. S. Nisar, A. N. Alharbi, R. Chouikh, Radiation effect on MHD Casson fluid flow over an inclined non-linear surface with chemical reaction in a Forchheimer porous medium, *Alexandria Engineering Journal,* Vol. 61, No. 10, pp. 8207-8220, 2022.

[16]   M. Senapati, K. Swain, S. K. Parida, Numerical analysis of three-dimensional MHD flow of Casson nanofluid past an exponentially stretching sheet, *Karbala Int. J. Mod. Sci,* Vol. 6, No. 1, pp. 93-102, 2020.

[17]   M. Senapati, S. K. Parida, K. Swain, S. M. Ibrahim, Analysis of variable magnetic field on chemically dissipative MHD boundary layer flow of Casson fluid over a nonlinearly stretching sheet with slip conditions, *International Journal of Ambient Energy*, pp. 1-15, 2020.

[18]   L. Panigrahi, J. Panda, K. Swain, G. C. Dash, Heat and mass transfer of MHD Casson nanofluid flow through a porous medium past a stretching sheet with Newtonian heating and chemical reaction, *Karbala Int J Mod Sci,* Vol. 6, No. 3, pp. 11, 2020.

[19]   S. Sahu, D. Thatoi, K. Swain, *Darcy-Forchheimer Flow Over a Stretching Sheet with Heat Source Effect: A Numerical Study*, in: *Recent Advances in Mechanical Engineering*, Eds., pp. 615-622: Springer, 2023.

[20]   M. M. Biswal, K. Swain, G. C. Dash, K. Ojha, Study of radiative magneto-non-Newtonian fluid flow over a nonlinearly elongating sheet with Soret and Dufour effects, *Numerical Heat Transfer, Part A: Applications*, pp. 1-12, 2022.

[21]   K. Swain, S. K. Parida, G. C. Dash, Effects of non-uniform heat source/sink and viscous dissipation on MHD boundary layer flow of Williamson nanofluid through porous medium, in *Proceeding of,* Trans Tech Publ, pp. 110-127.

[22]   M. V. Krishna, Chemical reaction, heat absorption and Newtonian heating on MHD free convective Casson hybrid nanofluids past an infinite oscillating vertical porous plate, *International Communications in Heat and Mass Transfer,* Vol. 138, pp. 106327, 2022.

[23]   M. Azam, T. Xu, M. Nayak, W. A. Khan, M. Khan, Gyrotactic microorganisms and viscous dissipation features on radiative Casson nanoliquid over a moving cylinder with activation energy, *Waves in Random and Complex Media*, pp. 1-23, 2022.

[24]   K. Sakkaravarthi, P. B. A. Reddy, Entropy generation on Casson hybrid nanofluid over a curved stretching sheet with convective boundary condition: Semi-analytical and numerical simulations, *Proceedings of the Institution of Mechanical Engineers, Part C: Journal of Mechanical Engineering Science*, pp. 09544062221119055, 2022.

[25]   S. Rao, P. Deka, A numerical solution using EFDM for unsteady MHD radiative Casson nanofluid flow over a porous stretching sheet with stability analysis, *Heat Transfer,* Vol. 51, No. 8, pp. 8020-8042, 2022.

[26]   M. Mohammadi, A. Farajpour, A. Moradi, M. Hosseini, Vibration analysis of the rotating multilayer piezoelectric Timoshenko nanobeam, *Engineering Analysis with Boundary Elements,* Vol. 145, pp. 117-131, 2022.

[27]   M. Mohammadi, A. Rastgoo, Primary and secondary resonance analysis of FG/lipid nanoplate with considering porosity distribution based on a nonlinear elastic medium, *Mechanics of Advanced Materials and Structures,* Vol. 27, No. 20, pp. 1709-1730, 2020.

[28]   M. Mohammadi, M. Hosseini, M. Shishesaz, A. Hadi, A. Rastgoo, Primary and secondary resonance analysis of porous functionally graded nanobeam resting on a nonlinear foundation subjected to mechanical and electrical loads, *European Journal of Mechanics-A/Solids,* Vol. 77, pp. 103793, 2019.

[29]   M. Mohammadi, A. Rastgoo, Nonlinear vibration analysis of the viscoelastic composite nanoplate with three directionally imperfect porous FG core, *Structural Engineering and Mechanics, An Int'l Journal,* Vol. 69, No. 2, pp. 131-143, 2019.

[30]   A. Farajpour, A. Rastgoo, M. Mohammadi, Vibration, buckling and smart control of microtubules using piezoelectric nanoshells under electric voltage in thermal environment, *Physica B: Condensed Matter,* Vol. 509, pp. 100-114, 2017.

[31]   A. Farajpour, M. H. Yazdi, A. Rastgoo, M. Loghmani, M. Mohammadi, Nonlocal nonlinear plate model for large amplitude vibration of magneto-electro-elastic nanoplates, *Composite Structures,* Vol. 140, pp. 323-336, 2016.

[32]   A. Farajpour, M. Yazdi, A. Rastgoo, M. Mohammadi, A higher-order nonlocal strain gradient plate model for buckling of orthotropic nanoplates in thermal environment, *Acta Mechanica,* Vol. 227, No. 7, pp. 1849-1867, 2016.

[33]   M. Mohammadi, M. Safarabadi, A. Rastgoo, A. Farajpour, Hygro-mechanical vibration analysis of a rotating viscoelastic nanobeam embedded in a visco-Pasternak elastic medium and in a nonlinear thermal environment, *Acta Mechanica,* Vol. 227, No. 8, pp. 2207-2232, 2016.

[34]   M. R. Farajpour, A. Rastgoo, A. Farajpour, M. Mohammadi, Vibration of piezoelectric nanofilm-based electromechanical sensors via higher-order non-local strain gradient theory, *Micro & Nano Letters,* Vol. 11, No. 6, pp. 302-307, 2016.

[35]   M. Baghani, M. Mohammadi, A. Farajpour, Dynamic and stability analysis of the rotating nanobeam in a nonuniform magnetic field considering the surface energy, *International Journal of Applied Mechanics,* Vol. 8, No. 04, pp. 1650048, 2016.

[36]   M. Goodarzi, M. Mohammadi, M. Khooran, F. Saadi, Thermo-mechanical vibration analysis of FG circular and annular nanoplate based on the visco-pasternak foundation, *Journal of Solid Mechanics,* Vol. 8, No. 4, pp. 788-805, 2016.

[37]   H. Asemi, S. Asemi, A. Farajpour, M. Mohammadi, Nanoscale mass detection based on vibrating piezoelectric ultrathin films under thermo-electro-mechanical loads, *Physica E: Low-dimensional Systems and Nanostructures,* Vol. 68, pp. 112-122, 2015.

[38] M. Safarabadi, M. Mohammadi, A. Farajpour, M. Goodarzi, Effect of surface energy on the vibration analysis of rotating nanobeam, 2015.

[39] M. Goodarzi, M. Mohammadi, A. Gharib, Techno-Economic Analysis of Solar Energy for Cathodic Protection of Oil and Gas Buried Pipelines in Southwestern of Iran, in *Proceeding of,* https://publications.waset.org/abstracts/33008/techno-economic-analysis-of …*,* pp.

[40] M. Mohammadi, A. A. Nekounam, M. Amiri, The vibration analysis of the composite natural gas pipelines in the nonlinear thermal and humidity environment, in *Proceeding of,* https://civilica.com/doc/540946/*,* pp.

[41] M. Goodarzi, M. Mohammadi, M. Rezaee, Technical Feasibility Analysis of PV Water Pumping System in Khuzestan Province-Iran, in *Proceeding of,* https://publications.waset.org/abstracts/18930/technical-feasibility …*,* pp.

[42] M. Mohammadi, A. Farajpour, A. Moradi, M. Ghayour, Shear buckling of orthotropic rectangular graphene sheet embedded in an elastic medium in thermal environment, *Composites Part B: Engineering,* Vol. 56, pp. 629-637, 2014.

[43] M. Mohammadi, A. Moradi, M. Ghayour, A. Farajpour, Exact solution for thermo-mechanical vibration of orthotropic mono-layer graphene sheet embedded in an elastic medium, *Latin American Journal of Solids and Structures,* Vol. 11, pp. 437-458, 2014.

[44] M. Mohammadi, A. Farajpour, M. Goodarzi, F. Dinari, Thermo-mechanical vibration analysis of annular and circular graphene sheet embedded in an elastic medium, *Latin American Journal of Solids and Structures,* Vol. 11, pp. 659-682, 2014.

[45] M. Mohammadi, A. Farajpour, M. Goodarzi, Numerical study of the effect of shear in-plane load on the vibration analysis of graphene sheet embedded in an elastic medium, *Computational Materials Science,* Vol. 82, pp. 510-520, 2014.

[46] A. Farajpour, A. Rastgoo, M. Mohammadi, Surface effects on the mechanical characteristics of microtubule networks in living cells, *Mechanics Research Communications,* Vol. 57, pp. 18-26, 2014.

[47] S. R. Asemi, M. Mohammadi, A. Farajpour, A study on the nonlinear stability of orthotropic single-layered graphene sheet based on nonlocal elasticity theory, *Latin American Journal of Solids and Structures,* Vol. 11, pp. 1541-1546, 2014.

[48] M. Goodarzi, M. Mohammadi, A. Farajpour, M. Khooran, Investigation of the effect of pre-stressed on vibration frequency of rectangular nanoplate based on a visco-Pasternak foundation, 2014.

[49] S. Asemi, A. Farajpour, H. Asemi, M. Mohammadi, Influence of initial stress on the vibration of double-piezoelectric-nanoplate systems with various boundary conditions using DQM, *Physica E: Low-dimensional Systems and Nanostructures,* Vol. 63, pp. 169-179, 2014.

[50] S. Asemi, A. Farajpour, M. Mohammadi, Nonlinear vibration analysis of piezoelectric nanoelectromechanical resonators based on nonlocal elasticity theory, *Composite Structures,* Vol. 116, pp. 703-712, 2014.

[51] M. Mohammadi, M. Ghayour, A. Farajpour, Free transverse vibration analysis of circular and annular graphene sheets with various boundary conditions using the nonlocal continuum plate model, *Composites Part B: Engineering,* Vol. 45, No. 1, pp. 32-42, 2013.

[52] M. Mohammadi, M. Goodarzi, M. Ghayour, A. Farajpour, Influence of in-plane pre-load on the vibration frequency of circular graphene sheet via nonlocal continuum theory, *Composites Part B: Engineering,* Vol. 51, pp. 121-129, 2013.

[53] M. Mohammadi, A. Farajpour, M. Goodarzi, R. Heydarshenas, Levy type solution for nonlocal thermo-mechanical vibration of orthotropic mono-layer graphene sheet embedded in an elastic medium, *Journal of Solid Mechanics,* Vol. 5, No. 2, pp. 116-132, 2013.

[54] M. Mohammadi, A. Farajpour, M. Goodarzi, H. Mohammadi, Temperature Effect on Vibration Analysis of Annular Graphene Sheet Embedded on Visco-Pasternak Foundati, *Journal of Solid Mechanics,* Vol. 5, No. 3, pp. 305-323, 2013.

[55] M. Danesh, A. Farajpour, M. Mohammadi, Axial vibration analysis of a tapered nanorod based on nonlocal elasticity theory and differential quadrature method, *Mechanics Research Communications,* Vol. 39, No. 1, pp. 23-27, 2012.

[56] A. Farajpour, A. Shahidi, M. Mohammadi, M. Mahzoon, Buckling of orthotropic micro/nanoscale plates under linearly varying in-plane load via nonlocal continuum mechanics, *Composite Structures,* Vol. 94, No. 5, pp. 1605-1615, 2012.

[57] M. Mohammadi, M. Goodarzi, M. Ghayour, S. Alivand, Small scale effect on the vibration of orthotropic plates embedded in an elastic medium and under biaxial in-plane pre-load via nonlocal elasticity theory, 2012.

[58]   A. Farajpour, M. Mohammadi, A. Shahidi, M. Mahzoon, Axisymmetric buckling of the circular graphene sheets with the nonlocal continuum plate model, *Physica E: Low-dimensional Systems and Nanostructures,* Vol. 43, No. 10, pp. 1820-1825, 2011.

[59]   A. Farajpour, M. Danesh, M. Mohammadi, Buckling analysis of variable thickness nanoplates using nonlocal continuum mechanics, *Physica E: Low-dimensional Systems and Nanostructures,* Vol. 44, No. 3, pp. 719-727, 2011.

[60]   H. Moosavi, M. Mohammadi, A. Farajpour, S. Shahidi, Vibration analysis of nanorings using nonlocal continuum mechanics and shear deformable ring theory, *Physica E: Low-dimensional Systems and Nanostructures,* Vol. 44, No. 1, pp. 135-140, 2011.

[61]   M. Mohammadi, M. Ghayour, A. Farajpour, Analysis of free vibration sector plate based on elastic medium by using new version differential quadrature method, *Journal of solid mechanics in engineering,* Vol. 3, No. 2, pp. 47-56, 2011.

[62]   A. Farajpour, M. Mohammadi, M. Ghayour, Shear buckling of rectangular nanoplates embedded in elastic medium based on nonlocal elasticity theory, in *Proceeding of,* www.civilica.com/Paper-ISME19-ISME19_390.html, pp. 390.

[63]   M. Mohammadi, A. Farajpour, A. R. Shahidi, Higher order shear deformation theory for the buckling of orthotropic rectangular nanoplates using nonlocal elasticity, in *Proceeding of,* www.civilica.com/Paper-ISME19-ISME19_391.html, pp. 391.

[64]   M. Mohammadi, A. Farajpour, A. R. Shahidi, Effects of boundary conditions on the buckling of single-layered graphene sheets based on nonlocal elasticity, in *Proceeding of,* www.civilica.com/Paper-ISME19-ISME19_382.html, pp. 382.

[65]   M. Mohammadi, M. Ghayour, A. Farajpour, Using of new version integral differential method to analysis of free vibration orthotropic sector plate based on elastic medium, in *Proceeding of,* www.civilica.com/Paper-ISME19-ISME19_497.html, pp. 497.

[66]   N. Ghayour, A. Sedaghat, M. Mohammadi, Wave propagation approach to fluid filled submerged visco-elastic finite cylindrical shells, 2011.

[67]   M. Mohammadi, A. Farajpour, A. Rastgoo, Coriolis effects on the thermo-mechanical vibration analysis of the rotating multilayer piezoelectric nanobeam, *Acta Mechanica*, https://doi.org/10.1007/s00707-022-03430-0, 2023.

[68]   W. Ibrahim, O. Makinde, Magnetohydrodynamic stagnation point flow and heat transfer of Casson nanofluid past a stretching sheet with slip and convective boundary condition, *Journal of Aerospace Engineering,* Vol. 29, No. 2, pp. 04015037, 2016.

[69]   W. Ibrahim, O. Makinde, Magnetohydrodynamic stagnation point flow of a power-law nanofluid towards a convectively heated stretching sheet with slip, *Proceedings of the Institution of Mechanical Engineers, Part E: Journal of Process Mechanical Engineering,* Vol. 230, No. 5, pp. 345-354, 2016.

[70]   O. Makinde, W. Khan, Z. Khan, Stagnation point flow of MHD chemically reacting nanofluid over a stretching convective surface with slip and radiative heat, *Proceedings of the Institution of Mechanical Engineers, Part E: Journal of Process Mechanical Engineering,* Vol. 231, No. 4, pp. 695-703, 2017.

[71]   P. Narayana, N. Tarakaramu, O. D. Makinde, B. Venkateswarlu, G. Sarojamma, MHD stagnation point flow of viscoelastic nanofluid past a convectively heated stretching surface, in *Proceeding of,* Trans Tech Publ, pp. 106-120.

[72]   M. Malik, O. Makinde, Parabolic curve fitting study subject to Joule heating in MHD thermally stratified mixed convection stagnation point flow of Eyring-Powell fluid induced by an inclined cylindrical surface, *Journal of King Saud University-Science,* Vol. 30, No. 4, pp. 440-449, 2018.

[73]   R. Mehmood, M. Nayak, N. S. Akbar, O. Makinde, Effects of thermal-diffusion and diffusion-thermo on oblique stagnation point flow of couple stress Casson fluid over a stretched horizontal Riga plate with higher order chemical reaction, *Journal of Nanofluids,* Vol. 8, No. 1, pp. 94-102, 2019.

[74]   K. Das, P. R. Duari, P. K. Kundu, Nanofluid flow over an unsteady stretching surface in presence of thermal radiation, *Alexandria engineering journal,* Vol. 53, No. 3, pp. 737-745, 2014.

[75]   K. Swain, S. Parida, G. Dash, MHD heat and mass transfer on stretching sheet with variable fluid properties in porous medium, *AMSE J Model B,* Vol. 86, pp. 706-726, 2017.

[76]   H. Schlichting, J. Kestin, 1961, *Boundary layer theory*, Springer,

[77]   M. Reza, A. Gupta, Shear flow over a rotating porous plate subjected to suction or blowing, *Physics of Fluids,* Vol. 19, No. 7, pp. 073601, 2007.